Structural but not functional connectivity differences within default mode network indicate conversion to dementia.

Lidón **Marin-Marin**[a], Anna **Miró-Padilla**[a], Víctor **Costumero**[a]*

[a]Neuropsychology and Functional Neuroimaging Group, Department of Basic Psychology, Clinical Psychology and Psychobiology. University Jaume I. 12071, Castelló, Spain

*** Correspondence:**

Víctor Costumero

vcostume@uji.es

+34 964 387655

Running title: DMN structural changes predict AD conversion.

ABSTRACT

Background: Malfunctioning of the default mode network (DMN) has been consistently related to mild cognitive impairment (MCI) and Alzheimer's disease (AD). However, evidence on differences in this network between MCI converters (MCI-c) and non-converters (MCI-nc), which could mark progression to AD, is still inconsistent. Objective: To multimodally investigate the DMN in the AD continuum. Methods: We measured gray matter (GM) volume, white matter (WM) integrity, and functional connectivity (FC) at rest in healthy elderly controls, MCI-c, MCI-nc and AD patients, matched on sociodemographic variables. Results: Significant differences between AD patients and controls were found in the structure of most of the regions of the DMN. MCI-c only differed from MCI-nc in GM volume of the left parahippocampus and bilateral hippocampi and middle frontal gyri, as well as in WM integrity of the parahippocampal cingulum connecting the left hippocampus and precuneus. We found significant correlations between integrity in some of those regions and global neuropsychological status, as well as an excellent

discrimination ability between converters and non-converters for the sum of GM volume of left parahippocampus, bilateral hippocampi and middle frontal gyri and WM integrity of left parahippocampal cingulum. However, we found no significant differences in FC. Conclusion: These results further support the relationship between abnormalities in the DMN and AD, and suggest that structural measures could be more accurate than resting-state estimates as markers of conversion from MCI to AD.

KEYWORDS: dementia, mild cognitive impairment, fMRI, atrophy, default mode network

INTRODUCTION

Alzheimer's disease (AD) is increasingly conceptualized as a disconnection syndrome, involving not only gray matter (GM) atrophy and accumulation of pathological proteins in specific brain regions, but also disrupted functioning of brain networks [1,2]. Alterations in functional connectivity (FC) have been found in the default mode (DMN), salience, and limbic networks, in patients with AD and mild cognitive impairment (MCI) [3]. However, recent studies tend to focus on the study of the DMN, since AD has been shown to especially affect the functioning of this network [4]. Namely, there seems to be a spatial overlap between DMN abnormalities and AD histopathology [5]. The DMN is characterized by being active in the brain at rest and becoming deactivated when a task is performed, indicating a state of alertness but not active involvement in a task [4]. Some of its components, such as the parietal, posterior cingulate, and precuneus, are associated with recollection [6], memory retrieval and consolidation [7]. Evidence shows structural white matter (WM) deterioration in AD patients in fibers connecting DMN nodes [2,8], and an accelerated aging pattern of DMN disconnection in AD patients compared to age-matched controls, with decreases in resting-state FC between its nodes [9,10]. Also importantly, resting-state FC abnormalities in the DMN have been shown to increase with disease severity [11]. Although neuropathology in the DMN seems to be consistently found in AD, the reason why this happens remains unknown [5,12]. The "metabolism hypothesis", suggests that the DMN's continuous high baseline activity increases the cascade that leads to dementia pathology [13], while others suggest that the DMN, among other multimodal networks, is associated with multiple cognitive functions and supports the integration of information, being especially vulnerable to early and fast spread of pathology for that very reason [14].

When investigating brain network alterations in MCI, studies report DMN abnormalities similar to those found in dementia patients, but to a lesser extent – that is, with integrity values that fall between those of dementia patients and healthy elderly controls [10]. MCI patients have also been found to show lower FC between hippocampi and posterior cingulate cortex (PCC) compared to healthy elderly controls [15], decreased whole-brain connectivity in PCC and precuneus [16], reduced connectivity between DMN nodes and between regions of the cortico-striatal-thalamic loop [17] and decreases in FC within the DMN and between the hippocampus and the DMN [18]. Regarding WM structure, a meta-analysis reported reliable abnormalities in WM integrity in MCI

patients in the fornix, uncinate fasciculus and parahippocampal cingulum [19], further confirmed by later studies [2,18].

All this evidence suggests that DMN alterations are typically implicated in both AD and MCI. However, it is estimated that 85-90% of MCI cases per year remain stable and do not progress to AD [20]. It is therefore relevant to identify the neural substrates that differentiate MCI converters (MCI-c) from non-converters (MCI-nc), which could mark deterioration leading to AD. Previous studies have linked medial temporal atrophy to progression from MCI to AD [21,22]. As for structural connectivity, previous investigations focusing on WM integrity have found significant differences between MCI-c and MCI-nc in the corpus callosum [23], and uncinate fasciculus [24], and reported thalamus [22], left hippocampus and cingulate [25], and bilateral corticospinal, right hippocampal cingulum, right inferior fronto-occipital, left inferior longitudinal, right superior longitudinal and left uncinate fasciculi integrity values as predictors of progression [26]. Regarding FC, a study found a significant predictive effect of a goodness-of-fit index of the DMN (i.e., the degree to which DMN maps of MCI patients matched those of controls), on progression from MCI to AD [27]. Based on this evidence, a general overview arises on GM structure markers of disease progression, which seem relatively consistent. However, to the best of our knowledge, evidence on WM integrity and resting-state FC, although abundant, still seems to be comparatively less consistent.

Considering this, the main objective of our study was to determine the contribution of brain alterations in the DMN to conversion from MCI to AD. With this aim, we carried out a multimodal study, focusing on a sample of MCI-c, MCI-nc, AD patients and healthy elderly control participants. We compared measures of three neuroimaging modalities between the groups: GM volume, WM integrity, and resting-state FC. Our hypothesis was that MCI-c would show significantly lower WM integrity than MCI-nc in fibers corresponding to the left hippocampus and cingulum, lower GM volume in the medial temporal lobe, and lower FC within the DMN. We also expected to find the same pattern when comparing AD patients to healthy controls. Finally, we also explored how AD-related alterations within the neuroimaging modalities related to global neuropsychological status.

MATERIALS AND METHODS

Participants

One hundred and three elderly individuals were recruited for this study, all of them selected from dementia units of the Valencian Community public healthcare system. Our sample consisted of 20 healthy elderly subjects (11 women; mean age=73.15, SD=4.45), 20 patients with a diagnosis of probable AD (13 women; mean age=74.95, SD=2.95), 31 patients with MCI that converted to dementia (22 women; mean age=74.26; SD=6.10) and 32 that did not convert (16 women; mean age=73.22, SD=4.98). MCI patients were classified as converters or non-converters after a follow-up with periodic neuropsychological assessments and clinical interviews every 6 months, although MR data was acquired only in the first clinical visit. Those who received a probable AD diagnosis during the follow-up - within a period of two years after the functional magnetic resonance imaging (MRI) session - were considered converters (MCI-c), whereas patients who remained stable after this period were classified as non-converters (MCI-nc).

Probable AD and MCI diagnoses were performed by experienced neurologists, based on clinical criteria. The participants of the AD group met revised criteria for probable AD [28] and showed a Clinical Dementia Rating (CDR) [29] score of 1 (mild AD). The inclusion criteria for the MCI group included 1) memory complaints, self-reported or confirmed by an informant; 2) objective memory impairment assessed with the logical memory subtest II from the Wechsler memory scale-III (WMS III) [30]; 3) essentially intact activities in daily living; 4) no evidence of dementia; and 5) a score of 0.5 on the CDR. All MCI patients were type amnestic. The healthy control group included participants that had no memory complaints, showed no impairment in their performance on the neuropsychological assessment, and a CDR score of 0. Criteria that implied exclusion from the study were the following: (1) suffering from other nervous system diseases such as a brain tumor, cerebrovascular disease, encephalitis, or epilepsy, or meeting the criteria for other dementia different from AD; (2) a score higher than 6 on the Geriatric Depression Scale [31,32] (3) visible abnormalities in magnetic resonance images, such as leukoaraiosis and infarction, reported by an experienced radiologist; and (4) suffering from a current psychiatric disorder or using psychoactive medication.

All participants were informed of the nature of the research, and provided written informed consent before their participation in the study. All study procedures were approved by the Ethics

Committee of the Universitat Jaume I of Castelló and conformed to the Code of Ethics of the World Medical Association (Declaration of Helsinki).

Neuropsychological assessment

Participants underwent a structured clinical interview and a neuropsychological assessment measuring language, memory, and general cognitive impairment, which included: a short form of the Boston Naming test (BNT) [33], a Word List Acquisition and Recall test (immediate and delayed recall), two Fluency tests (semantic and phonetic), a remote memory test, and the clock-drawing test [34]. With the purpose of simplification, a composite global neuropsychological score was calculated by obtaining the mean of the standardized values of the measures. See Table 1 for details on sociodemographic variables (gender, age and years of schooling) and neuropsychological performance of the four groups.

MRI acquisition

Images were acquired on a 3T MRI scanner (Siemens Magnetom Trio, Erlangen, Germany), using a 12-channel head coil. Participants were placed in a supine position inside the scanner, and their heads were immobilized with cushions to reduce motion. Whole-brain 3-D images were collected using sagittal T1-weighted images (MPRAGE sequence, 176 slices, 256x256 matrix, TR=2300 ms, TE=2.98 ms, flip angle=9º, spatial resolution 1x1x1 mm). Axial diffusion tensor images (DTI) were acquired with an echo-planar imaging sequence (EPI) with 20 gradient directions, with the following scan parameters: TR = 10300 ms, TE = 104 ms, b0/b = 0/1000s/mm2, FOV = 256 mm, matrix = 128x128, flip angle = 90º, number of slices = 70, slice thickness = 2 mm, gap = 0mm. Finally, during the resting-state functional imaging acquisition, participants were instructed to just rest with their eyes closed, trying to let their minds go blank and not to fall asleep. A total of 270 volumes were collected over 9 min using a gradient-echo T2*-weighted echo-planar imaging sequence (TR=2000 ms; TE=30 ms; matrix, 64 x 64; FOV, 224 x 224 cm; flip angle, 90°; 33 slices, parallel to the hippocampus; slice thickness, 3.5 mm; slice gap, 0.5 mm).

Image preprocessing and analyses

Region-based morphometry analysis

Structural GM analyses were performed with CAT12 (Computational Anatomy Toolbox; C. Gaser, Jena University Hospital, Jena, Germany; http://dbm.neuro.uni-jena.de/cat/) using their standard preprocessing pipeline. A first quality check was conducted to detect images affected by important inhomogeneity or movement artefacts. After an initial bias correction of intensity non-uniformities, individual volumes of GM, WM, and cerebrospinal fluid were estimated applying segmentation, and images were registered to the shooting template provided in the CAT12 toolbox. Then, the region of interest (ROI) analysis implemented in CAT12 was performed. In this analysis, also called Region-based morphometry (RBM), a mask in standard space is transformed into native subject space, and the sum of the local GM inside the mask is estimated. We restricted our analysis to the nodes of the dorsal and ventral DMN characterized in Shirer's 2012 atlas [35] (i.e., dorsal DMN: precuneus, left and right hippocampus, left and right medial frontal cortex, left and right angular gyri, midcingulate cortex, thalamus; ventral DMN: left and right retrosplenial cortex, left and right middle frontal gyrus, left and right parahippocampal gyri, left and right middle occipital gyri, dorsal precuneus and right cerebellum – lobe IX).

DTI analysis

All DTI data were processed using the FMRIB Software Library (FSL) [36]. Diffusion weighted images were corrected for eddy current distortions using *eddycorrect*, brain extraction and deletion of non-brain tissue were performed using *bet* (Brain Extraction Tool) [37], and *dtifit* was applied to extract fractional anisotropy (FA), mean diffusivity (MD), axial diffusivity (AxD) and radial diffusivity (RD). Tract-based spatial statistics of FA, MD, AxD, and RD was carried out using TBSS [38]. Non-linear registration of all FA individual images to a common space was performed using the tool FNIRT (https://fsl.fmrib.ox.ac.uk/fsl/fslwiki/FNIRT), and a mean FA skeleton was created and thinned in order to represent the center of all tracts common to the subjects. Finally, each subject's aligned FA data were projected onto this skeleton. The same process was used for MD, AxD, and RD. We calculated the mean FA, MD, AxD and RD of those fibers connecting the dorsal and ventral DMN, based on a probabilistic DTI atlas [39] of fMRI-guided tractography

between previously defined DMN nodes [35]. We focused on the streamlines with a probability of 25% or higher of belonging to the DMN, following the procedure of a previous study [40]. Seven streamlines obtained less than 50 voxels and were excluded from further analyses. Ten fibers of interest remained, connecting the following nodes: (a) precuneus – left hippocampus; (b) precuneus – right hippocampus; (c) left medial frontal cortex – precuneus; (d) left medial frontal cortex – midcingulate cortex; (e) left medial frontal cortex – thalamus; (f) precuneus – midcingulate cortex; (g) thalamus – left hippocampus; (h) left – right retrosplenial cortex; (i) left middle occipital gyrus – dorsal precuneus; (j) right retrosplenial cortex – dorsal precuneus.

ROI to ROI resting-state FC analysis

We used Data Processing and Analysis for Brain Imaging (DPABI V4.2_190919, http://rfmri.org/dpabi) to carry out resting-state data processing. Preprocessing included: (1) removal of the first ten volumes of each raw dataset; (2) slice timing correction; (3) realignment using a six-parameter (rigid body) linear transformation; (4) spatial normalization to the Montreal Neurological Institute (MNI) space (voxel size 3 × 3 × 3 mm); (5) removal of spurious variance through linear regression: 24 parameters from the head motion correction, linear, and quadratic trends, and the first five principal components associated with WM and cerebrospinal fluid [41]; (6) spatial smoothing with a 4-mm FWHM Gaussian Kernel; and (7) band-pass temporal filtering (0.01–0.1 Hz). None of the participants had more than 2 mm/degree of movement in any of the six directions or fewer than 120 volumes with framewise displacement (FD) < 0.5 mm [42], ensuring at least 4 minutes of rest with low FD. Moreover, there were no significant differences between the groups in FD. ROI time courses were extracted from regions of the DMN [35], then FC between ROIs was estimated using Pearson's correlation and r to z transformation was applied using the Fisher's method. We focused our analyses on the connectivity between the regions linked by the fibers of interest of our DTI analyses (i.e., precuneus, left and right hippocampus, left medial frontal cortex, midcingulate cortex, thalamus, left and right retrosplenial cortex, left middle occipital gyrus and dorsal precuneus). To avoid the introduction of different amounts of noise derived from the signal average of regions with different sizes, we used the centroids of the ROIs provided on the atlas [35] to create spherical masks (5mm radius) as our seeds. We visually inspected the spheres to verify that they were representative of each brain region – i.e., that voxels

of the sphere did not fall out of the ROI. Specifically, we used the following MNI coordinates as centers of the spheres: precuneus (1, -53, 28), left (-24, -29, -13) and right (27, -23, -17) hippocampus, left medial frontal cortex (-3, 49, 14), midcingulate cortex (3, -15, 36), thalamus (-1, -8, 4), left (-12, -58, 15) and right (13, -53, 15) retrosplenial cortex, left middle occipital gyrus (-36 -81 32) and dorsal precuneus (1 -57 54). Additionally, FC between dorsal and ventral DMN nodes not linked by the fibers of interest of our DTI analyses was also explored.

Statistical analyses

Group differences in GM volume, WM diffusion and ROI to ROI resting-state FC were investigated with Kruskal-Wallis tests. Statistical threshold was set at $p<0.05$ and the family-wise error (FWE) rate was corrected using the Bonferroni method. Planned post hoc comparisons between AD-healthy controls and MCI-c-MCI-nc were performed for each significant result using Mann-Whitney U test. All the analyses were performed in SPSS 23 (IBM Corp.). When using GM volumes, TIV was corrected using the power proportion method [43] as implemented in R (https://github.com/tkoscik/tkmisc).

We estimated post-hoc correlations in SPSS 23 to explore the relationship between modality estimates in regions that showed to be relevant for conversion from MCI to AD and global neuropsychological score. For DTI measures, we used bivariate Pearson's correlations, and for GM volumes, we used partial correlations controlling for TIV. These analyses were restricted to participants that presented a disease (MCI-c, MCI-nc and AD).

Finally, receiver operator curves (ROC) and their area under these curve (AUC) were calculated for the modality estimates in regions that turned out to be relevant for conversion, for their combination, and for the composite global neuropsychological score, in order to assess their ability to discriminate between the categories of MCI-c and MCI-nc. The sign of RD values was reversed in order to transform them to the same discriminative direction as GM volume values. GM volumes were corrected for TIV using the power proportion method [43] as implemented in R (https://github.com/tkoscik/tkmisc), and a mean of the two hemispheres was used for hippocampus and middle frontal gyrus. Following up on a previous study [44], logistic regression analysis was used to combine the measures relevant for conversion in a single ROC. Confidence intervals and

asymptotic significance were calculated, considering true area = 0.5 as the null hypothesis. Youden's index for rating diagnostic tests [45,46] was used to determine the most appropriate cut-off value for the evaluated measures, maximizing the sum of sensitivity and specificity.

RESULTS

Sociodemographic and neuropsychological variables

We found significant differences between the groups in all neuropsychological measures and the global neuropsychological score, but there were no significant differences in proportion of men and women, age or years of schooling (Table 1).

Table 1. Sociodemographic and neuropsychological variables of the four groups.

	Healthy elderly (N = 20)		**MCI non-converters** (N = 32)		**MCI Converters** (N = 31)		**AD patients** (N = 20)		Statistical differences	P
Gender	M/W = 9/11		M/W = 16/16		M/W = 9/22		M/W = 7/13		$\chi2 = 3.31$	0.347
	M	SD	M	SD	M	SD	M	SD	F	
Age	73.15	4.45	73.22	4.98	74.26	6.10	74.95	2.95	0.71	0.551
Years of schooling	8.15	2.73	8.41	3.14	9.10	3.74	8.63	4.10	0.26	0.855
BNT	11.95	0.22	9.78	1.00	8.87	1.69	7.40	3.02	25.31	<0.001
Phonetic Fluency	13.20	2.02	9.44	1.39	8.23	2.63	4.95	2.96	45.50	<0.001
Semantic Fluency	17.05	2.87	11.31	1.87	10.06	3.37	7.70	3.16	40.12	<0.001
Immediate recall	6.50	0.57	2.85	0.57	3.04	1.03	1.85	1.22	109.62	<0.001
Delayed recall	6.65	0.75	1.22	0.42	1.03	1.07	0.20	0.52	328.40	<0.001
Remote memory	11.70	1.34	9.47	0.92	9.39	1.54	5.65	2.56	48.97	<0.001
Clock drawing test	9	0	7.38	1.19	6.55	1.69	4.05	2.82	30.34	<0.001
Global NPS score	1.33	0.23	0.00	0.19	-0.21	0.46	-1.04	0.67	113.79	<0.001

BNT, Boston Naming Test; NPS, neuropsychological; N, sample size; M/W, men/women; $\chi2$, chi-squared test; M, Mean; SD, Standard Deviation; F, F value for ANOVA.

Region-based morphometry analysis

We found significant differences between the groups in GM values of the left and right hippocampus (left: H=27.56, p<0.001, FWE-corrected; right: H=26.13, p<0.001, FWE-corrected), left and right parahippocampus (left: H=27.22, p<0.001, FWE-corrected; right: H=25.82, p<0.001, FWE-corrected) and left and right middle frontal gyrus (left: H=16.97, p=0.014, FWE-corrected; right: H=15.64, p<0.025, FWE-corrected). In post hoc two-sample analyses, we found that these results were driven by AD patients showing lower GM volume than elderly controls (left hippocampus: U=39, p<0.001; right hipppocampus: U=65, p<0.001; left parahippocampus: U=58,

p<0.001; right parahippocampus: U=31, p<0.001; left middle frontal gyrus: U=92, p=0.006; right middle frontal gyrus: U=105, p=0.02; Fig. 1) and MCI-c showing lower GM volumes than MCI-nc (left hippocampus: U=299, p=0.014; right hippocampus: U=267, p=0.003; left parahippocampus: U=260, p=0.002; left middle frontal gyrus: U=312, p=0.023; right middle frontal gyrus: F=293, p=0.011; Fig. 1). Finally, we also found significant positive correlations between the global neuropsychological score and GM volumes in left hippocampus (R=0.231, p=0.037) and left parahippocampus (R=0.369, p<0.001) in patients (MCI-c, MCI-nc and AD).

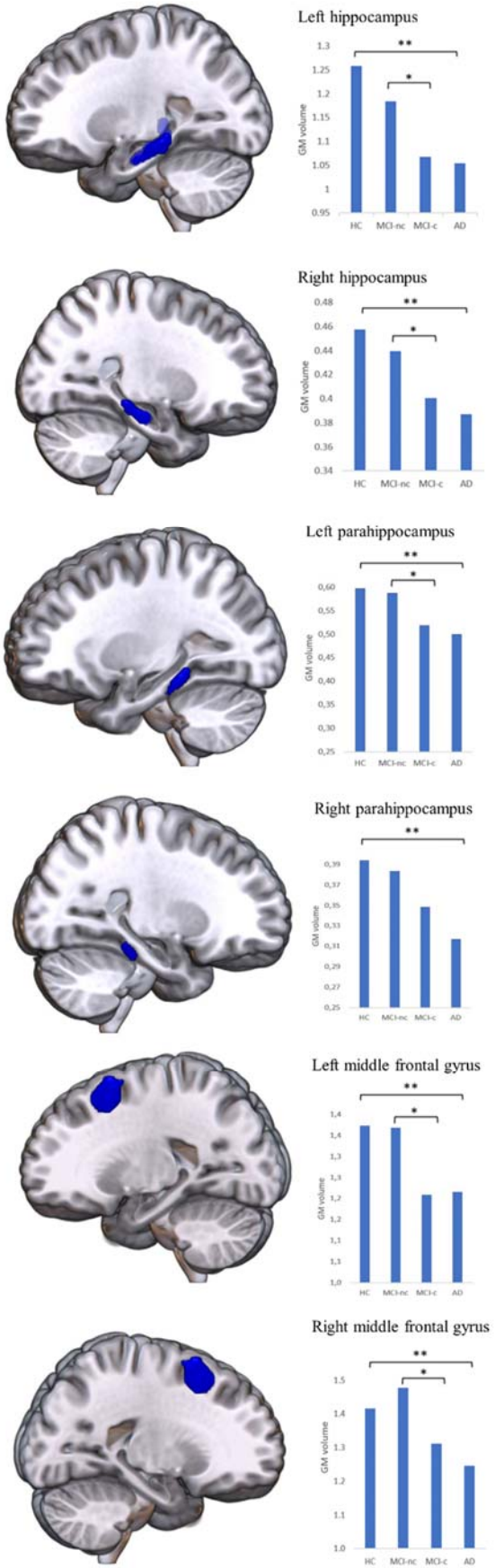

Figure 1. GM volume (mm3) differences between healthy elderly controls, MCI-c, MCI-nc and AD patients. Asterisks indicate significant differences (* at a threshold of $p<0.05$, FWE-corrected; ** $p<0.01$ FWE-corrected).

DTI analysis

We found significant differences between the groups in all DTI measures and fibers of the DMN, except for the tracts connecting the left medial frontal and midcingulate cortices, the left and right retrosplenial cortices and left middle occipital gyrus and dorsal precuneus (see Supplementary Material for details). In post hoc two sample analyses, we found that these differences were the aftereffect of AD patients showing lower WM integrity than healthy elderly controls. We also found that MCI-c showed higher MD and RD than MCI-nc in the WM fiber linking the precuneus and left hippocampus, the left parahippocampal cingulum (MD: U=301, p=0.015, FWE-corrected; RD: U=298, p=0.013, FWE-corrected; Figure 2). Finally, MD and RD of the parahippocampal cingulum significantly negatively correlated with the global neuropsychological score in patients (MD: R=-0.334, p=0.002; RD: R=-0.315, p=0.004).

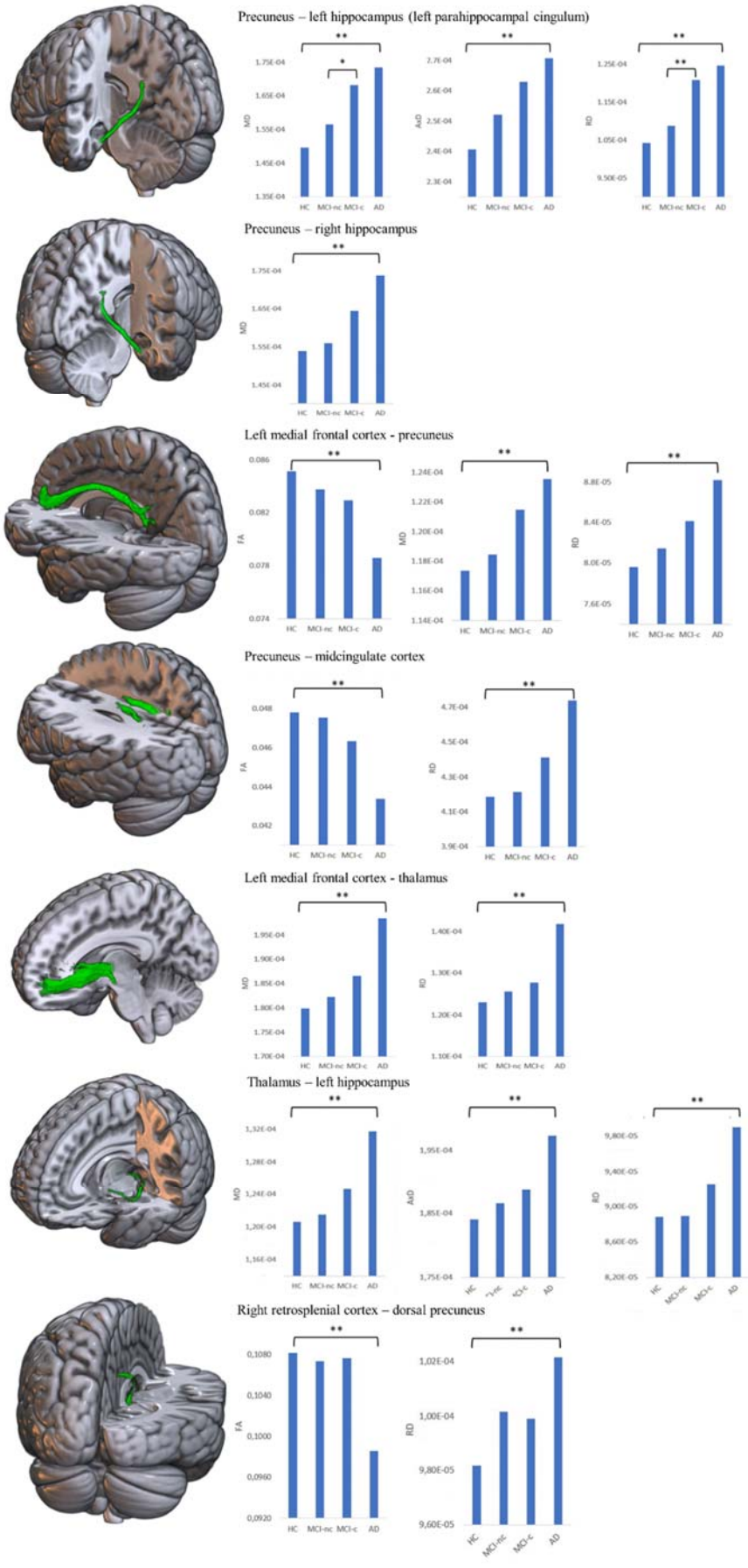

Figure 2. WM integrity differences between healthy elderly controls, MCI-c, MCI-nc and AD patients. Asterisks indicate significant differences (* at a threshold of $p<0.05$, FWE-corrected; ** $p<0.01$ FWE-corrected).

ROI to ROI resting-state FC analysis

We found no significant differences between the groups in FC between DMN regions using the predefined threshold of $p < 0.05$ FWE-corrected. However, considering uncorrected results, differences in FC between the precuneus and left hippocampus ($H=11.06$, $p=0.011$ uncorrected), among others, were observed. This effect was driven by lower FC in AD patients than healthy controls. FC analysis between DMN nodes not linked by the fibers of interest of our DTI analyses yielded no significant results. Uncorrected results are reported in Supplementary Material – Figure 1.

ROC analysis

For GM measures, we calculated ROCs and AUCs separately for regions that turned out to be relevant for conversion (bilateral middle frontal gyri and hippocampi, and left parahippocampus) and for their combination. The combination showed better discrimination between MCI-c and MCI-nc than each region separately (see Supplementary Material – Figure 2). Therefore, we used this conjoint measure in our definitive ROC analysis to compare discrimination ability between modalities. For DTI measures, we calculated ROCs and AUCs separately for MD and RD values of the tract connecting precuneus and left hippocampus. RD showed better discrimination between MCI-c and MCI-nc than MD (see Supplementary Material – Figure 3), so we used negative RD values as WM measures for this analysis. The ROC for discrimination between MCI-c and MCI-nc of GM and WM measures, their combination and global neuropsychological score are shown in Figure 3. The global neuropsychological score showed an AUC of 0.722 (SE=0.067, p=0.001, lower boundary=0.591, upper boundary=0.853). RD values of the left parahippocampal cingulum with inverted sign showed an AUC of 0.700 (SE=0.066, p=0.003, lower boundary=0.569, upper boundary=0.830). The combination of left parahippocampus and bilateral hippocampi and middle frontal gyri (i.e., GM measures) showed an AUC of 0.757 (SE=0.061, p=0.000, lower boundary=0.637, upper boundary=0.877). The combination of GM measures and DTI (RD values of left parahippocampal cingulum) showed an AUC of 0.804 (SE=0.056, p=0.000, lower boundary=0.695, upper boundary=0.914). Cut-off values estimated using Youden's approach, sensitivity and specificity for each of the measures are reported in Supplementary Material – Table 2.

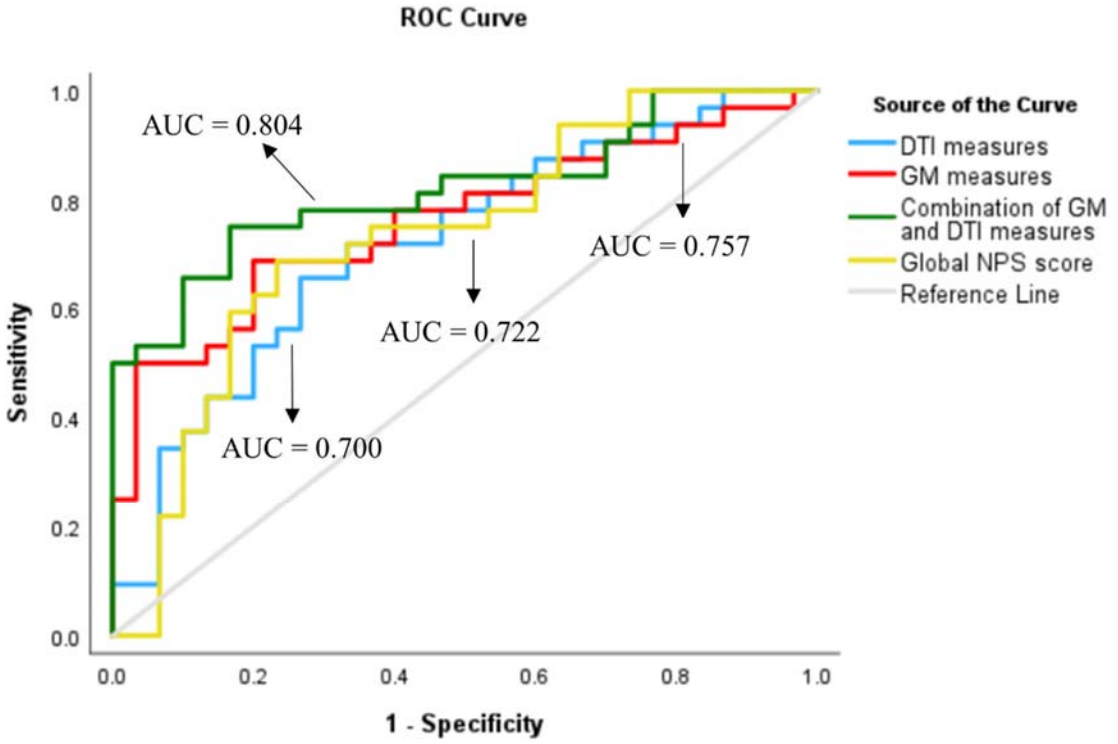

Figure 3. ROCs for DTI measures (WM integrity of left parahippocampal cingulum, i.e., negative RD values, in blue), GM measures (volumes of left parahippocampus and bilateral hippocampi and middle frontal gyri, in red), the combination of GM and DTI measures (in green), and the global neuropsychological score (in yellow), assessing their ability to discriminate between the categories of MCI-c and MCI-nc. ROC=receiver operator curve, AUC=area under the curve, GM=grey matter, DTI=diffusion tensor imaging, NPS=neuropsychological.

DISCUSSION

In this prospective multimodal MRI study, we investigated structural and functional alterations of the DMN as possible markers of transition from MCI to dementia. Specifically, we analyzed GM volume, WM integrity and FC of a single sample of elderly participants with similar age, years of schooling and proportion of men and women, that differed in their diagnoses: healthy elderly controls, MCI patients that converted to AD during a follow-up of two years, MCI that remained stable, and AD patients. Our analyses revealed that AD patients showed significantly lower WM integrity than elderly controls in most of the DMN fibers and lower GM volumes in bilateral hippocampi, parahippocampi and middle frontal gyri. MCI-c showed lower WM integrity than MCI-nc in the fiber connecting the precuneus and left hippocampus, and lower GM volume in left parahippocampus and bilateral hippocampi and middle frontal gyri, but no differences in FC within the DMN.

Our results are in agreement with previous findings of atrophy in the medial temporal lobe in AD patients, described since long [13]. Regarding progression from MCI to AD, our results coincide with previous evidence showing that MCI-c differ from MCI-nc in GM atrophy in medial temporal and frontal DMN regions [21,22]. Specifically, our results show that MCI patients that converted to AD in a period of two years or less had lower GM volumes in hippocampi, middle frontal gyri and left parahippocampus than those who did not convert. Moreover, GM volume of these regions emerged as a marker with acceptable ability of discrimination between MCI-c and MCI-nc, as measured by their area under the ROC [47]. We also found significant correlations between GM volume of left hippocampus and parahippocampus and global neuropsychological score in patients, which supports the relationship between atrophy of regions of the DMN and general cognitive impairment.

We also provide evidence supporting findings of WM density loss in the DMN [2] and reductions in the numbers of fibers connecting this network [8] in dementia, by showing that AD patients present lower WM integrity than healthy elderly participants between most of the nodes of the DMN as measured by all DTI measures. Crucially, we found that MCI-c presented lower integrity (higher MD and RD) in the fiber of DMN that connects the precuneus and left hippocampus, the left parahippocampal cingulum, which has been previously associated to episodic memory in MCI [48]. Previous evidence pointed towards the relevance of this fiber in conversion to AD: WM

integrity in left hippocampus and left cingulate had been previously described as predictor of disease progression [25] and FA reductions in MCI-c compared to healthy controls in the parahippocampal cingulum had also been found, but significant differences between MCI-c and MCI-nc in this tract were absent [49]. Therefore, we provide new evidence in favor of the relevance of the parahippocampal cingulum for conversion to AD. Notably, MD and RD were the only DTI measures that emerged as sensitive to MCI progression in the left parahippocampal cingulum, in agreement with previous evidence describing RD as the DTI metric that best discriminates between different stages of the disease [50]. Furthermore, MD and RD in the left parahippocampal cingulum showed an acceptable discrimination ability between MCI-c and MCI-nc [47] and correlated significantly with global neuropsychological score in patients, further corroborating its contribution to disease status and general cognitive function. Also noteworthy, the discrimination ability of RD in the left parahippocampal cingulum and GM in bilateral middle frontal gyri and hippocampi and left parahippocampus combined turned out to be excellent [47], better than the acceptable discrimination capacities obtained for them separately and for the global neuropsychological score, which supports the relevance of these structural measures as markers of conversion from MCI to AD.

Finally, our data goes in line with previous evidence showing that AD patients present lower resting-state FC between the precuneus and left medial temporal lobe [9,10,51], since the tendencies towards FC differences found in our sample between these regions, although uncorrected, were driven by differences between healthy controls and AD. Importantly, we found no significant differences between MCI-c and MCI-nc in FC in the DMN. A recent meta-analysis on resting-state FC studies investigating DMN abnormalities in MCI found substantial inconsistency and low replicability in results, which led them to conclude that DMN resting-state connectivity does not qualify as a useful biomarker of disease progression or AD risk [52], which could explain the lack of differences in FC between MCI-c and MCI-nc in our results. However, these negative results should be interpreted with caution. First, our analyses were restricted to DMN areas. Therefore, possible between groups FC differences in other brain areas were not considered. Furthermore, in order to favor comparability between DTI and FC measures we used seed to seed correlations as FC technique. However, AD related changes in the FC of DMN areas have been shown in other studies using more advanced techniques such as graph theory [53]. Thus,

the reported negative results for the FC analyses should be interpreted taking into consideration the methodological context of this study.

An additional explanation for the lack of significant differences in resting-state FC when comparing our MCI groups might be the sample size of our investigation. Although it is larger than the ones used in most previous studies, according to a previous meta-analysis [52], others affirm that sample sizes should exceed by far 100 in order to optimize replicability [54]. Finally, another limitation of our study is the lack of tau or amyloid measurements, which are recommended by the National Institute on Aging and Alzheimer's Association as biomarkers for AD and MCI diagnosis in research, in an attempt to focus the definition of the disease on the pathological processes rather than the symptoms [55]. However, the correspondence between the clinical syndrome of AD and the underlying pathologic process has been shown to be good, with 94.1% of patients with a clinical diagnosis of AD being in the AD-continuum [56], following NIA-AA's criteria based on biomarkers [55]. Moreover, all MCI patients of our sample were amnestic, the subtype of MCI most associated with progression to AD [57,58]. Thus, the results of this study might be useful not only to guide future AD research based on clinical symptoms but also studies using biomarkers.

In sum, our study shows that the structure of the DMN is widely altered in AD patients compared to controls. However, when measured at baseline, MCI patients that converted to AD during a 2 years' follow-up and those who remained stable only differed in GM integrity of bilateral middle frontal gyri and hippocampi, left parahippocampus, and its left WM connections with the precuneus, with no differences in resting-state FC between the nodes of the DMN. Therefore, our results support the notion that GM abnormalities of medial temporal and frontal DMN areas are key for disease progression, and adds new evidence regarding the relevance of WM integrity between the precuneus and left hippocampus for conversion from MCI to AD. Our evidence also supports the involvement of DMN abnormalities in dementia, but suggests that structural measures of GM and WM atrophy in the medial temporal lobe could work better than connectivity of the DMN as indicators of conversion from MCI to AD.

ACKNOWLEDGEMENTS

This work was supported by the project PID2019-105077RJ-I00 by State Research Agency of the Spanish Ministry of Science and Innovation (MCIN/AEI) /10.13039/501100011033, awarded to VC. AM-P was funded by the postdoctoral program POSDOC-2019-Universitat Jaume I (POSDOC/2019/01). LM-M was supported by an FPU grant from the Spanish Ministry of Education, Culture and Sports (FPU 17/00698).

CONFLICT OF INTEREST

The authors have no conflict of interest to report.

REFERENCES

[1] Brier MR, Thomas JB, Ances BM (2014) Network dysfunction in Alzheimer's disease: refining the disconnection hypothesis. *Brain Connect* **4**, 299–311.

[2] Mito R, Raffelt D, Dhollander T, Vaughan DN, Tournier JD, Salvado O, Brodtmann A, Rowe CC, Villemagne VL, Connelly A (2018) Fibre-specific white matter reductions in Alzheimer's disease and mild cognitive impairment. *Brain*.

[3] Badhwar AP, Tam A, Dansereau C, Orban P, Hoffstaedter F, Bellec P (2017) Resting-state network dysfunction in Alzheimer's disease: A systematic review and meta-analysis. *Alzheimer's Dement Diagnosis, Assess Dis Monit* **8**, 73–85.

[4] Mohan A, Roberto AJ, Mohan A, Lorenzo A, Jones K, Carney MJ, Liogier-Weyback L, Hwang S, Lapidus KAB (2016) The significance of the Default Mode Network (DMN) in neurological and neuropsychiatric disorders: A review. *Yale J Biol Med* **89**, 49–57.

[5] Dennis EL, Thompson PM (2014) Functional brain connectivity using fMRI in aging and Alzheimer's disease. *Neuropsychol Rev* **24**, 49–62.

[6] Vincent JL, Snyder AZ, Fox MD, Shannon BJ, Andrews JR, Raichle ME, Buckner RL (2006) Coherent spontaneous activity identifies a hippocampal-parietal memory network. *J Neurophysiol* **96**, 3517–3531.

[7] Buckner RL, Andrews-Hanna JR, Schacter DL (2008) The brain's default network: Anatomy, function, and relevance to disease. *Ann N Y Acad Sci* **1124**, 1–38.

[8] Tucholka A, Grau-Rivera O, Falcon C, Rami L, Sánchez-Valle R, Lladó A, Gispert JD, Molinuevo JL (2018) Structural connectivity alterations along the Alzheimer's disease continuum: Reproducibility across two independent samples and correlation with cerebrospinal fluid amyloid-β and tau. *J Alzheimer's Dis* **61**, 1575–1587.

[9] Wang L, Zang Y, He Y, Liang M, Zhang X, Tian L, Wu T, Jiang T, Li K (2006) Changes in hippocampal connectivity in the early stages of Alzheimer's disease: Evidence from resting state fMRI. *Neuroimage* **31**, 496–504.

[10] Binnewijzend MAA, Schoonheim MM, Sanz-Arigita E, Wink AM, van der Flier WM,

Tolboom N, Adriaanse SM, Damoiseaux JS, Scheltens P, van Berckel BNM, Barkhof F (2012) Resting-state fMRI changes in Alzheimer's disease and mild cognitive impairment. *Neurobiol Aging* **33**, 2018–2028.

[11] Wu X, Li R, Fleisher AS, Reiman EM, Guan X, Zhang Y, Chen K, Yao L (2011) Altered default mode network connectivity in alzheimer's disease-A resting functional MRI and bayesian network study. *Hum Brain Mapp* **32**, 1868–1881.

[12] Desgranges B, Mevel K, Chételat G, Eustache F (2011) The default mode network in healthy aging and Alzheimer's disease. *Int J Alzheimers Dis*.

[13] Buckner RL, Snyder AZ, Shannon BJ, LaRossa G, Sachs R, Fotenos AF, Sheline YI, Klunk WE, Mathis CA, Morris JC, Mintun MA (2005) Molecular, structural, and functional characterization of Alzheimer's disease: Evidence for a relationship between default activity, amyloid, and memory. *J Neurosci* **25**, 7709–7717.

[14] Mišić B, Betzel RF, Nematzadeh A, Goñi J, Griffa A, Hagmann P, Flammini A, Ahn YY, Sporns O (2015) Cooperative and Competitive Spreading Dynamics on the Human Connectome. *Neuron* **86**, 1518–1529.

[15] Sorg C, Riedl V, Mühlau M, Calhoun VD, Eichele T, Läer L, Drzezga A, Förstl H, Kurz A, Zimmer C, Wohlschläger AM (2007) Selective changes of resting-state networks in individuals at risk for Alzheimer's disease. *Proc Natl Acad Sci U S A* **104**, 18760–18765.

[16] Drzezga A, Becker JA, Van Dijk KRA, Sreenivasan A, Talukdar T, Sullivan C, Schultz AP, Sepulcre J, Putcha D, Greve D, Johnson KA, Sperling RA (2011) Neuronal dysfunction and disconnection of cortical hubs in non-demented subjects with elevated amyloid burden. *Brain* **134**, 1635–1646.

[17] Tam A, Dansereau C, Badhwar AP, Orban P, Belleville S, Chertkow H, Dagher A, Hanganu A, Monchi O, Rosa-Neto P, Shmuel A, Wang S, Breitner J, Bellec P (2015) Common effects of amnestic mild cognitive impairmenton resting-state connectivity across four independent studies. *Front Aging Neurosci* **7**,.

[18] Gilligan TM, Sibilia F, Farrell D, Lyons D, Kennelly SP, Bokde ALW (2019) No relationship between fornix and cingulum degradation and within-network decreases in

functional connectivity in prodromal Alzheimer's disease. *PLoS One* **14**,.

[19] Yu J, Lam CLM, Lee TMC (2017) White matter microstructural abnormalities in amnestic mild cognitive impairment: A meta-analysis of whole-brain and ROI-based studies. *Neurosci Biobehav Rev*.

[20] Roberts R, Knopman DS (2013) Classification and epidemiology of MCI. *Clin Geriatr Med* **29**, 753–772.

[21] DeCarli C, Frisoni GB, Clark CM, Harvey D, Grundman M, Petersen RC, Thal LJ, Jin S, Jack CR, Scheltens P (2007) Qualitative estimates of medial temporal atrophy as a predictor of progression from mild cognitive impairment to dementia. *Arch Neurol* **64**, 108–115.

[22] Brueggen K, Dyrba M, Barkhof F, Hausner L, Filippi M, Nestor PJ, Hauenstein K, Klöppel S, Grothe MJ, Kasper E, Teipel SJ (2015) Basal forebrain and hippocampus as predictors of conversion to Alzheimer's disease in patients with mild cognitive impairment-a multicenter DTI and volumetry study. *J Alzheimer's Dis* **48**, 197–204.

[23] van Bruggen T, Stieltjes B, Thomann PA, Parzer P, Meinzer HP, Fritzsche KH (2012) Do Alzheimer-specific microstructural changes in mild cognitive impairment predict conversion? *Psychiatry Res - Neuroimaging* **203**, 184–193.

[24] Hiyoshi-Taniguchi K, Oishi N, Namiki C, Miyata J, Murai T, Cichocki A, Fukuyama H (2015) The Uncinate Fasciculus as a Predictor of Conversion from Amnestic Mild Cognitive Impairment to Alzheimer Disease. *J Neuroimaging* **25**, 748–753.

[25] Marcos Dolado A, Gomez-Fernandez C, Yus Fuertes M, Barabash Bustelo A, Marcos-Arribas L, Lopez-Mico C, Jorquera Moya M, Fernandez-Perez C, Montejo Carrasco P, Cabranes Diaz JA, Arrazola Garcia J, Maestu Unturbe F (2019) Diffusion Tensor Imaging Measures of Brain Connectivity for the Early Diagnosis of Alzheimer's Disease. *Brain Connect* **9**, 594–603.

[26] Stone DB, Ryman SG, Hartman AP, Wertz CJ, Vakhtin AA (2021) Specific White Matter Tracts and Diffusion Properties Predict Conversion From Mild Cognitive Impairment to Alzheimer's Disease. *Front Aging Neurosci* **13**,.

[27] Petrella JR, Sheldon FC, Prince SE, Calhoun VD, Doraiswamy PM (2011) Default mode network connectivity in stable vs progressive mild cognitive impairment. *Neurology* **76**, 511–517.

[28] McKhann GM, Knopman DS, Chertkow H, Hyman BT, Jack CR, Kawas CH, Klunk WE, Koroshetz WJ, Manly JJ, Mayeux R, Mohs RC, Morris JC, Rossor MN, Scheltens P, Carrillo MC, Thies B, Weintraub S, Phelps CH (2011) The diagnosis of dementia due to Alzheimer's disease: Recommendations from the National Institute on Aging-Alzheimer's Association workgroups on diagnostic guidelines for Alzheimer's disease. *Alzheimer's Dement* **7**, 263–269.

[29] Morris JC (1997) Clinical Dementia Rating: A reliable and valid diagnostic and staging measure for dementia of the Alzheimer type. In *International Psychogeriatrics* Int Psychogeriatr, pp. 173–176.

[30] Wechsler D (1997) *Wechsler Adult Intelligence Scale-Third Edition*, The Psychological Corporation., San Antonio, TX.

[31] Martínez de la Iglesia J, Onís Vilches MC, Dueñas Herrero R, Albert Colomer C, Aguado Taberné C, Luque Luque R (2002) *The Spanish version of the Yesavage abbreviated questionnaire (GDS) to screen depressive dysfunc-tions in patients older than 65 years*.

[32] Yesavage JA, Brink TL, Rose TL, Lum O, Huang V, Adey M, Leirer VO (1982) Development and validation of a geriatric depression screening scale: A preliminary report. *J Psychiatr Res* **17**, 37–49.

[33] Serrano C, Allegri RF, Drake M, Butman J, Harris P, Nagle C, Ranalli C (2001) Versión abreviada en español del test de denominación de Boston: Su utilidad en el diagnóstico diferencial de la enfermedad de Alzheimer. *Rev Neurol* **33**, 624–627.

[34] Cacho J, García-García R, Arcaya J, Gay J, Guerrero-Peral AL, Gómez-Sánchez JC, Vicente JL (1996) The "clock drawing test" in healthy elderly people. *Rev Neurol* **24**, 1525–8.

[35] Shirer WR, Ryali S, Rykhlevskaia E, Menon V, Greicius MD (2012) Decoding subject-driven cognitive states with whole-brain connectivity patterns. *Cereb Cortex* **22**, 158–165.

[36] Smith SM, Jenkinson M, Woolrich MW, Beckmann CF, Behrens TEJ, Johansen-Berg H, Bannister PR, De Luca M, Drobnjak I, Flitney DE, Niazy RK, Saunders J, Vickers J, Zhang Y, De Stefano N, Brady JM, Matthews PM (2004) Advances in functional and structural MR image analysis and implementation as FSL. *Neuroimage* **23**, 208–219.

[37] Smith SM (2002) Fast robust automated brain extraction. *Hum Brain Mapp* **17**, 143–155.

[38] Smith SM, Jenkinson M, Johansen-Berg H, Rueckert D, Nichols TE, Mackay CE, Watkins KE, Ciccarelli O, Cader MZ, Matthews PM, Behrens TEJ (2006) Tract-based spatial statistics: Voxelwise analysis of multi-subject diffusion data. *Neuroimage*.

[39] Figley TD, Bhullar N, Courtney SM, Figley CR (2015) Probabilistic atlases of default mode, executive control and salience network white matter tracts: An fMRI-guided diffusion tensor imaging and tractography study. *Front Hum Neurosci* **9**, 585.

[40] Prillwitz CC, Rüber T, Reuter M, Montag C, Weber B, Elger CE, Markett S (2018) The salience network and human personality: Integrity of white matter tracts within anterior and posterior salience network relates to the self-directedness character trait. *Brain Res* **1692**, 66–73.

[41] Behzadi Y, Restom K, Liau J, Liu TT (2007) A component based noise correction method (CompCor) for BOLD and perfusion based fMRI. *Neuroimage* **37**, 90–101.

[42] Jenkinson M, Bannister P, Brady M, Smith S (2002) Improved optimization for the robust and accurate linear registration and motion correction of brain images. *Neuroimage* **17**, 825–841.

[43] Liu D, Johnson HJ, Long JD, Magnotta VA, Paulsen JS (2014) The power-proportion method for intracranial volume correction in volumetric imaging analysis. *Front Neurosci* **8**,.

[44] Liu K, Chen K, Yao L, Guo X (2017) Prediction of Mild Cognitive Impairment Conversion Using a Combination of Independent Component Analysis and the Cox Model. *Front Hum Neurosci* **11**, 33.

[45] Youden WJ (1950) Index for rating diagnostic tests. *Cancer* **3**, 32–35.

[46] Habibzadeh F, Habibzadeh P, Yadollahie M (2016) On determining the most appropriate test cut-off value: the case of tests with continuous results. *Biochem Medica* **26**, 297.

[47] Hosmer DW, Lemeshow S, Sturdivant RX, Army Academy US (2013) Applied Logistic Regression Third Edition.

[48] Metzler-Baddeley C, Hunt S, Jones DK, Leemans A, Aggleton JP, O'Sullivan MJ (2012) Temporal association tracts and the breakdown of episodic memory in mild cognitive impairment. *Neurology* **79**, 2233–2240.

[49] Ito K, Sasaki M, Takahashi J, Uwano I, Yamashita F, Higuchi S, Goodwin J, Harada T, Kudo K, Terayama Y (2015) Detection of early changes in the parahippocampal and posterior cingulum bundles during mild cognitive impairment by using high-resolution multi-parametric diffusion tensor imaging. *Psychiatry Res Neuroimaging* **231**, 346–352.

[50] Becerra-Laparra I, Cortez-Conradis D, Garcia-Lazaro H, Martinez-Lopez M, Roldan-Valadez E (2020) Radial Diffusivity is the Best Global Biomarker Able to Discriminate Healthy Elders, Mild Cognitive Impairment, and Alzheimer's Disease: A Diagnostic Study of DTI-Derived Data. *Neurol India* **68**, 427–434.

[51] Greicius MD, Srivastava G, Reiss AL, Menon V (2004) Default-mode network activity distinguishes Alzheimer's disease from healthy aging: Evidence from functional MRI. *Proc Natl Acad Sci U S A* **101**, 4637–4642.

[52] Eyler LT, Elman JA, Hatton SN, Gough S, Mischel AK, Hagler DJ, Franz CE, Docherty A, Fennema-Notestine C, Gillespie N, Gustavson D, Lyons MJ, Neale MC, Panizzon MS, Dale AM, Kremen WS (2019) Resting State Abnormalities of the Default Mode Network in Mild Cognitive Impairment: A Systematic Review and Meta-Analysis. *J Alzheimer's Dis* **70**, 107–120.

[53] Costumero V, d'Oleire Uquillas F, Diez I, Andorrà M, Basaia S, Bueichekú E, Ortiz-Terán L, Belloch V, Escudero J, Ávila C, Sepulcre J (2020) Distance disintegration delineates the brain connectivity failure of Alzheimer's disease. *Neurobiol Aging* **88**, 51–60.

[54] Turner BO, Paul EJ, Miller MB, Barbey AK (2018) Small sample sizes reduce the

replicability of task-based fMRI studies. *Commun Biol* **1**, 1–10.

[55] Jack CR, Bennett DA, Blennow K, Carrillo MC, Dunn B, Haeberlein SB, Holtzman DM, Jagust W, Jessen F, Karlawish J, Liu E, Molinuevo JL, Montine T, Phelps C, Rankin KP, Rowe CC, Scheltens P, Siemers E, Snyder HM, Sperling R, Elliott C, Masliah E, Ryan L, Silverberg N (2018) NIA-AA Research Framework: Toward a biological definition of Alzheimer's disease. *Alzheimer's Dement* **14**, 535–562.

[56] Carandini T, Arighi A, Sacchi L, Fumagalli GG, Pietroboni AM, Ghezzi L, Colombi A, Scarioni M, Fenoglio C, De Riz MA, Marotta G, Scarpini E, Galimberti D (2019) Testing the 2018 NIA-AA research framework in a retrospective large cohort of patients with cognitive impairment: From biological biomarkers to clinical syndromes. *Alzheimer's Res Ther* **11**, 1–11.

[57] Yaffe K, Petersen RC, Lindquist K, Kramer J, Miller B (2006) Subtype of mild cognitive impairment and progression to dementia and death. *Dement Geriatr Cogn Disord* **22**, 312–319.

[58] Jungwirth S, Zehetmayer S, Hinterberger M, Tragl KH, Fischer P (2012) The validity of amnestic MCI and non-amnestic MCI at age 75 in the prediction of Alzheimer's dementia and vascular dementia. *Int psychogeriatrics* **24**, 959–966.

AUTHOR CONTRIBUTIONS

Victor Costumero: Conceptualization (lead), data curation (lead), formal analysis (supporting), funding acquisition (lead), project administration (lead), supervision (lead), writing – original draft preparation (supporting), writing – review and editing (equal). Anna Miró-Padilla: Conceptualization (supporting), data curation (supporting), formal analysis (supporting), project administration (supporting), supervision (supporting), visualization (supporting), writing – original draft preparation (supporting), writing - review and editing (equal). Lidón Marin-Marin: formal analysis (lead), methodology (lead), project administration (supporting), visualization (lead), writing – original draft preparation (lead), writing - review and editing (equal).

DATA AVAILABILITY STATEMENT

The data that support the findings of this study are available on request from the corresponding author. The data are not publicly available due to privacy or ethical restrictions.

Supplementary Material

Structural but not Functional Connectivity Differences within Default Mode Network Indicate Conversion to Dementia

Supplementary Table 1. Differences between the groups in all DTI measures and fibers of the DMN using Kruskal-Wallis test (significant results in bold).

DMN fibers	DTI measures	H Statistic	p FWE corrected
Precuneus – left hippocampus (left parahippocampal cingulum)	FA	7.14	>0.1
	MD	**21.91**	**<0.001**
	AxD	**20.30**	**0.002**
	RD	**18.32**	**0.004**
Precuneus – right hippocampus	FA	7.39	>0.1
	MD	**14.56**	**0.022**
	AxD	11.47	0.091
	RD	12.49	0.057
Left medial frontal cortex - precuneus	**FA**	**12.87**	**0.048**
	MD	**12.82**	**0.049**
	AxD	5.19	>0.1
	RD	**14.25**	**0.026**
Precuneus – midcingulate cortex	**FA**	**19.56**	**0.002**
	MD	11.28	0.098
	AxD	1.56	>0.1
	RD	**15.36**	**0.015**
Left medial frontal cortex – midcingulate cortex	FA	8.08	>0.1
	MD	5.35	>0.1
	AxD	5.60	>0.1
	RD	6.92	>0.1
Left medial frontal cortex - thalamus	FA	11.38	>0.1
	MD	11.78	0.079
	AxD	8.79	>0.1
	RD	**12.83**	**0.049**
Thalamus – left hippocampus	FA	8.92	>0.1
	MD	**18.14**	**0.004**
	AxD	**16.29**	**0.010**
	RD	**16.67**	**0.008**
Left – right retrosplenial cortex	FA	9.96	>0.1
	MD	8.70	>0.1
	AxD	4.42	>0.1
	RD	11.11	>0.1
Left middle occipital gyrus – dorsal precuneus	FA	10.21	>0.1
	MD	11.87	0.076
	AxD	5.35	>0.1
	RD	12.12	0.068
Right retrosplenial cortex – dorsal precuneus	FA	11.90	0.075
	MD	10.69	>0.1
	AxD	3.21	>0.1
	RD	**13.55**	**0.035**

Supplementary Table 2. Youden's index, cut-off value, and sensitivity and specificity estimates for each of the four models in the ROC analysis.

Measure	Youden's index (Se + Sp -1)	Sensitivity	1-Specificity	Cut-off value
DTI	0.366	0.656	0.290	-0.00011437
GM	0.462	0.688	0.226	0.5356209
Global NPS score	0.440	0.656	0.226	-0.523
GM + DTI	0.556	0.750	0.194	0.5275129

Se, sensitivity; Sp, specificity; DTI, diffusion tensor imaging, refers to left PH cingulum integrity (negative RD values); GM, grey matter, refers to regional volumes; NPS, neuropsychological

Supplementary Figure 1. Uncorrected results for analysis of FC between the regions linked by both the fibers of interest of our DTI analyses and those not linked by them. Asterisks indicate significant post-hoc Mann-Whitney's U tests at $p<0.05$ threshold.

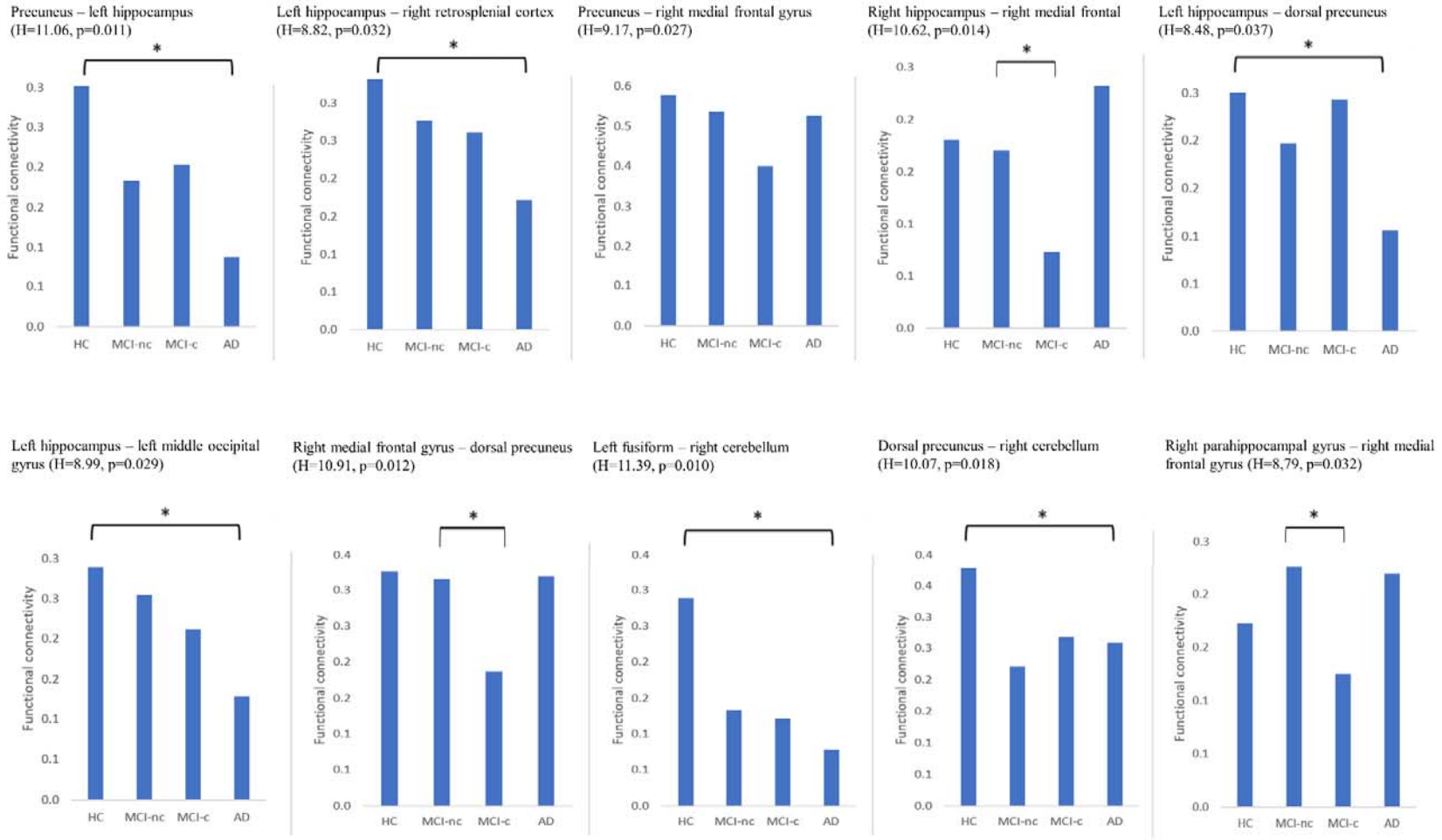

Supplementary Figure 2. ROCs and AUCs for GM volumes of bilateral hippocampus, left parahippocampus and bilateral middle frontal gyrus separately, and for their combination, assessing their ability to discriminate between the categories of MCI-c and MCI-nc. ROC, receiver operator curve; AUC, area under the curve.

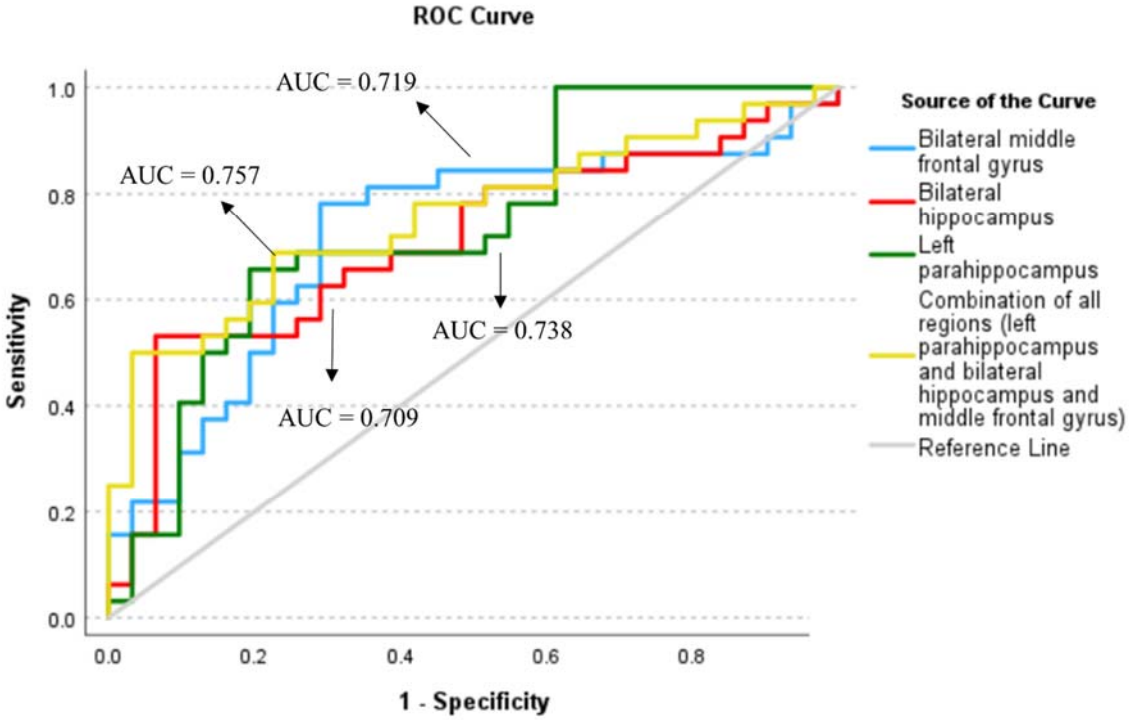

Supplementary Figure 3. ROCs and AUCs for negative MD and RD values in the WM fiber linking the precuneus and left hippocampus, assessing their ability to discriminate between the categories of MCI-c and MCI-nc. ROC, receiver operator curve; AUC, area under the curve.